

## Chapter 17

# Engineering Earthquake Early Warning via Regional Networks

I. Iervolino

**Abstract** Significant investments are undergoing internationally to develop earthquake early warning (EEW) systems. So far, reasonably, the most of the research in this field was driven by seismologists as the issues to determine essential feasibility of EEW were mainly related to the earthquake source. Many of them have been brilliantly solved, and the principles of this discipline are collected in the so-called *real-time seismology*. On the other hand, operating EEW systems rely on general-purpose intensity measures as proxies for the impending ground motion potential and suitable for population alert. In fact, to date, comparatively little attention was given to EEW by earthquake engineering, and design approaches for structure-specific EEW are mostly lacking. Applications to site-specific systems have not been extensively investigated and EEW convenience is not yet proven except a few pioneering cases, although the topic is certainly worthwhile. For example, in structure-specific EEW the determination of appropriate alarm thresholds is important when the false alarm may induce significant losses; similarly, economic appeal with respect to other risk mitigation strategies, as seismic upgrade, should be assessed. In the paper the least issues to be faced in the design of engineering applications of EEW are reviewed and some work done in this direction is discussed. The review presented intends to summarize the work of the author and co-workers in this field illustrating a possible *performance-based* approach for the design of structure-specific applications of EEW.

---

This invited paper is a shortened version of the review of the work of the author and related research group given in Iervolino (2011).

---

I. Iervolino (✉)

Dipartimento di Strutture per l'Ingegneria e l'Architettura, Università di Napoli Federico II,  
Via Claudio, 21, 80125 Naples, Italy  
e-mail: iunio.iervolino@unina.it

## 17.1 Introduction

At a large scale, the basic elements of an earthquake early warning (EEW) system are seismic instruments (individual or multiple arranged in form of a network), a processing unit for the data measured by the sensors, and a transmission infrastructure spreading the alarm to the end users (Heaton 1985). This alarm may trigger security measures (manned or automated), which are expected to reduce the seismic risk in real-time; i.e., before the strong ground motion reaches the warned site. In fact, from the engineering point of view, an EEW system may be appealing for specific structures only if it is competitive cost-wise and/or if it allows to achieve some seismic performance traditional risk mitigation strategies cannot. EEW may be particularly useful in all those situations when some ongoing activity may be profitably interrupted, or posed in a safe mode, in the case of an earthquake to prevent losses (i.e., a *security action* is undertaken). This is the case for example, of facilities treating hazardous materials as nuclear power plants or gas distribution systems. In the first case, the reactor can be temporarily protected before the earthquake hits, in the second case distribution may be interrupted until it is verified that damages and releases potentially triggering fires and explosions did not occur. In these situations it is clear that the early warning, which is in principle only a piece of *information* regarding the earthquake, represents the input for a local protection system. Simpler, yet potentially effective, applications are related to manned operations as surgery in hospitals or the protection from injuries due to fall of non-structural elements in buildings. EEW information seems less suitable to reduce the risk directly related to structural damage (although some potential application may be conceived); in any case, it has to be proven that they are more convenient than more traditional seismic protection systems.

Two points, not usually faced by earthquake engineering, emerge then: (i) because effective engineering applications of EEW involve shutdown of valuable operations and the downtime is very costly for production facilities, unnecessary stops (*false alarms*) should be avoided as much as possible; (ii) development of EEW applications basically deals with the *best* engineering use of seismological information provided in *real-time* on the approaching earthquake. In fact, the basic design variables for EEW applied to a specific engineered system are:

- the estimated earthquake potential on the basis of the EEW information;
- the available time before the earthquake to strike (*lead-time*);
- the system *performance* (proxy for the loss) associated to the case the alarm is issued, which may also include the cost of false alarm and depends on the chosen security action.

In the following, the work of the author and co-workers regarding these issues will be reviewed. It will be discussed below how these three items are not independent each other and that the whole involves very large uncertainty.

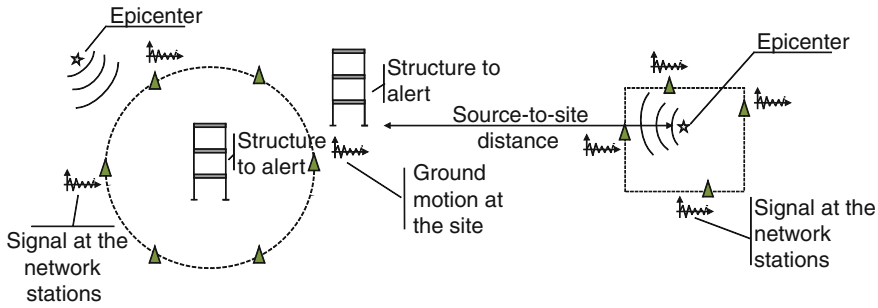


**Fig. 17.1** Site-specific (*left*), and hybrid (*right*) EEW schemes; modified from Iervolino et al. (2006)

## 17.2 Estimating Ground Motion Potential in Real-Time

Conceptually, EEW systems are often identified by the configuration of the seismic network, as *regional* or *site-specific* (Kanamori 2005).

Site-specific systems are devoted to enhance in real-time the safety margin of critical systems as nuclear power plants, lifelines or transportation infrastructures by automated safety actions (e.g., Veneziano and Papadimitriou (1998) and Wieland et al. (2000)). The networks for specific EEW cover the surroundings of the system creating a kind of a fence for the seismic waves (Fig. 17.1, left). The location of the sensors depends on the time needed to activate the safety procedures before the arrival of the more energetic seismic phase at the site (or *lead-time*). In these *Seismic Alert Systems* (Wieland 2001) the alarm is typically issued when the S-phase ground motion at one or more sensors exceeds a given threshold and there is no attempt to estimate the source features as magnitude ( $M$ ) and location because a local measure of the effects (i.e., the ground motion) is already available. In the *on-site* systems, the seismic sensors (one or more) are placed within the system to warn. In this case the ground damaging potential is typically estimated on the basis of the P-waves and the *lead-time* is given by the residual time for the damaging S-waves to arrive.

Regional EEWs consist of wide seismic networks covering a portion of the area which is likely to be the source of earthquakes. Data from regional networks are traditionally used for long term seismic monitoring or to estimate, right after the event (i.e., in *near-real-time*), territorial distributions of ground shaking obtained via spatial interpolation of records (e.g., *Shakemap* (Wald et al. 1999)) for emergency management. Regional infrastructures are usually available in seismic regions and are operated by governmental authorities; this is why the most of the ongoing research is devoted to exploit these systems for real-time alert use (Fig. 17.1, right) as a few examples attest (e.g., Doi (2010)). In fact, the work presented in the following mostly refers to the feasibility and design of structure-specific alert (i.e., as in site-specific systems), starting from estimating the peak ground motion at the site, using the sole information from regional networks, which consists of the estimation of source features as  $M$  and location of the earthquake. This was referred to as *hybridizing* the two EEW approaches (Iervolino et al. 2006).

### 17.2.1 Real-Time Probabilistic Seismic Hazard Analysis

In the framework of performance-based earthquake engineering or PBEE (Cornell and Krawinkler 2000) the earthquake potential, with respect to the performance demand for a structure, is estimated via the so-called probabilistic seismic hazard analysis or PSHA (Cornell 1968), which consists of the probability that a ground motion intensity measure (IM), likely to be a proxy for the destructive power of the earthquake, the peak ground acceleration (PGA) for example, is exceeded at the site of interest during the *service life* of the structure. This is done via Eq. (17.1), in which, referring for simplicity to a single earthquake source<sup>1</sup>:  $\lambda$  is the rate of occurrence of earthquakes on the source;  $f(m)$  is the probability density function, or PDF, of  $M$ ;  $f(r)$  is the PDF of the source-to-site-distance ( $R$ ); and  $f(im|m, r)$  is the PDF of IM given  $M$  and  $R$  (e.g., from a ground motion prediction equation or GMPE).

$$f(im) = \lambda \int_m \int_r f(im|m, r) f(m) f(r) dr dm \quad (17.1)$$

Because seismologists have recently developed several methods to estimate  $M$  and  $R$  in real-time while the event is still developing, for example from limited information of the P-waves, the PSHA approach can be adapted for earthquake early warning purposes. The so-called real-time PSHA or RTPSHA, introduced in Iervolino et al. (2006), tends to replace some of the terms in Eq. (17.1), with their real time counterparts.

It has been shown in Iervolino et al. (2007a) that if at a given time  $t$  from the earthquake's origin, the seismic network can provide a vector of measures informative for the magnitude,  $\{\tau_1, \tau_2, \dots, \tau_n\}$ , then the PDF of  $M$  conditional to the measures,  $f(m|\tau_1, \tau_2, \dots, \tau_n)$ , may be obtained via the Bayes theorem,<sup>2</sup> Eq. (17.2),

$$f(m|\tau_1, \tau_2, \dots, \tau_n) = k \cdot e^{\left[2 \cdot \mu_{\ln(\tau)} \cdot \left(\sum_{i=1}^n \ln(\tau_i)\right) - n \cdot \mu_{\ln(\tau)}^2\right] / 2 \cdot \sigma_{\ln(\tau)}^2} \cdot e^{-\beta m} \quad (17.2)$$

where  $\beta$  is a parameter depending on the Gutenberg-Richter relationship for the source and  $k$  is a constant.  $\mu_{\ln(\tau)}$  and  $\sigma_{\ln(\tau)}$  are the mean and standard deviation of the logs of the measure used to estimate  $M$  (e.g., from Allen and Kanamori (2003)). Note finally that the PDF of  $M$  in Eq. (17.2) depends on the real-time data only via

$n$  and  $\sum_{i=1}^n \ln(\tau_i)$ , which are related to the geometric mean,  $\hat{\tau} = \sqrt[n]{\prod_{i=1}^n \tau_i}$ .

Regarding  $R$ , because of rapid earthquake localization procedures (e.g., Satriano et al. (2008)), a probabilistic estimate of the epicenter may also be available based

<sup>1</sup> In Eq. (17.1) it is assumed for simplicity that  $M$  and  $R$  are independent random variables, which may not be the general case.

<sup>2</sup> It is to mention that simpler approaches to estimation of  $M$  can be implemented in the RTPSHA although the Bayesian one has proven to be the most efficient one (Iervolino et al. 2009).

on the sequence according to which the stations trigger,  $\{s_1, s_2, \dots, s_n\}$ . Thus, the real-time PDF of R,  $f(r|s_1, s_2, \dots, s_n)$ , may replace  $f(r)$  in Eq. (17.1). In fact, the PSHA hazard of Eq. (17.1), has its real-time adaption in Eq. (17.3). Because when the earthquake is already occurring the  $\lambda$  parameter does not apply, in principle, no further data are required to compute the PDF of the IM or, equivalently, the complementary cumulative distribution (or hazard curve) of IM at any site of interest. A simulation of RTPSHA for a magnitude 6 event is given in Fig. 17.2 referring to the *Irpinia Seismic Network* (ISNet, (Weber et al. 2007)) in Campania (southern Italy).

$$f(im|\underline{\tau}, \underline{s}) = \int_m \int_r f(im|m, r) f(m|\tau_1, \tau_2, \dots, \tau_n) f(r|s_1, s_2, \dots, s_n) dr dm \quad (17.3)$$

The figure shows that, because the knowledge level about the earthquake (i.e., M and R) increases as the seismic signals are processed by an increasing number of seismic sensors (i.e.,  $n$ ), the real-time hazard evolves with time. In Fig. 17.2 the panels (a), (b), and (c) show the number of stations of the network which have measured the parameter informative for the magnitude at three different instants from the earthquake origin time. In the (c) and (d) panels, the corresponding PDFs of M and R are given, while panel (e) shows the real-time hazard curves in which the IM considered is the PGA on stiff soil (computed using the GMPE of Sabetta and Pugliese (1996)). The three instants chosen correspond to when 2, 18 and 29 (the whole network) have recorded at least 4 s of the P-waves, which is the required time to estimate  $\tau$  according to Allen and Kanamori (2003). For further details on the simulation the reader should refer to Iervolino et al. (2006), Iervolino et al. (2007a), and Iervolino et al. (2009).

Note finally that, the RTPSHA can be easily extended to estimate in real-time the response spectrum ordinates, this has been done in Convertito et al. (2008).

### 17.2.2 Decisional Rules, Alarm Thresholds and False Alarm Probabilities

An essential engineering issue in earthquake early warning is the *alarming decisional rule*, which should be based on the consequences of the decision of alarming or not and is remarkably dependent both on the information gathered on the earthquake and on the system to alarm.

If RTPSHA is the approach used in the early warning system, the knowledge level about the earthquake at a certain time is represented by the hazard curve computed at that instant. The alarming decisional rule should be established based on that. The simplest is to alarm if the expected value of the considered IM is larger than a threshold, Eq.<sup>3</sup> (17.4).

<sup>3</sup> Conditional dependencies are dropped from the equations for simplicity.

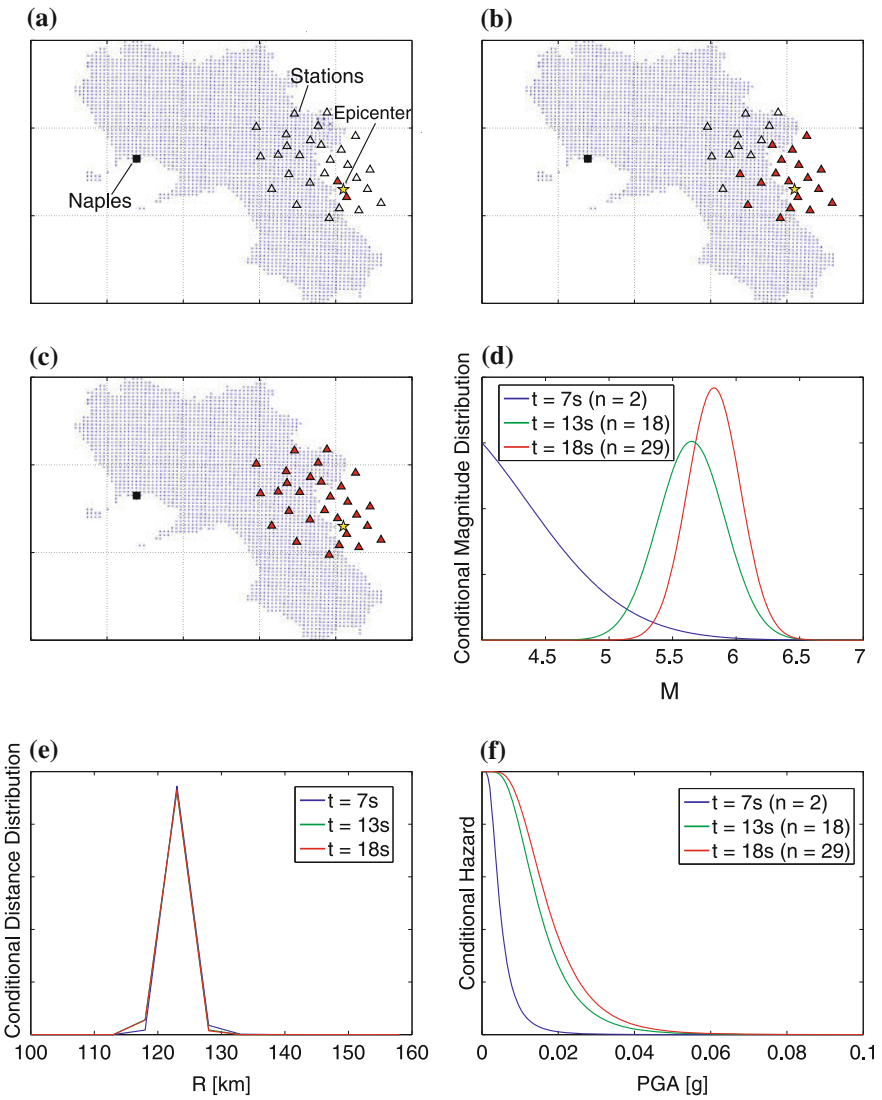


**Fig. 17.2** a–c seismic stations which have measured the parameter informative for the magnitude of the earthquake (i.e., 4 s of the P-wave velocity signal (Allen and Kanamori 2003)) at three different instants during the earthquake; d–f are the  $M$ ,  $R$  and PGA distributions computed at the same instants via the RTPSHA approach (modified from Iervolino et al. (2009))

$$E [IM] = \int_{-\infty}^{+\infty} im f(im) d(im) \geq im_c \quad (17.4)$$

The  $im_c$  threshold depends on the system to alarm. For example, if structural damage is the consequence, and the IM is the PGA, the  $PGA_c$  value should reflect the ground motion intensity above which damages for that specific structure are expected; e.g., the PGA value used for the design of the structure.

A more refined decisional rule, still based on the RTPSHA outcome, may be to alarm if the critical IM value has an *unacceptable* risk (represented by the probability value  $Pr_c$ ) of being exceeded in that earthquake, Eq. (17.5).

$$\Pr [IM > im_c] = 1 - \int_{-\infty}^{im_c} f(im) d(im) \geq Pr_c \quad (17.5)$$

This latter approach to the EEW alarming decision is similar to the earthquake resistant design in codes worldwide, where the design is carried out for an IM value corresponding to a fixed probability of exceedance in the lifetime of the structure (e.g., 10% in 50 years). In fact, Eq. (17.5) maybe seen as Eq. (17.6).

$$im(Pr_c) < im_c \quad (17.6)$$

This means that, if PGA is the IM, the alarm has to be issued if the PGA, which in the real-time hazard curve has the critical probability of being exceeded, is larger than the critical PGA for the structure.

The two rules of Eqs. (17.4) and (17.5) are represented in Fig. 17.3a where, for the PDF of PGA derived from the hazard curve at  $n = 29$  in Fig. 17.2, it is shown a case in which, for the specific  $im_c$  and  $Pr_c$  values, the alarm should be issued according to the first rule and should not according to the second one.

As discussed, the PDF of M may be seen as sole function of  $\hat{\tau} = \sqrt[n]{\prod_{i=1}^n \tau_i}$ ; moreover, as shown below, simply the modal value of R may adequately represent its PDF due to the negligible uncertainty involved in the earthquake location rapid estimation methods. Therefore, because the GMPE is a static piece (not depending on the real-time measures) of information, the RTPSHA integral may be computed offline for all possible values of the  $\hat{\tau}$  and R pair, and the result retrieved in real-time without the need for computing it. This is an attractive feature of the proposed approach for EEW purposes. As an example, in Table 17.1 the probabilities of exceedance are tabulated for the arbitrary  $PGA_c$  value of 0.017 g, using the GMPE of Sabetta and Pugliese (1996) and as a function of the two independent parameters required to compute the RTPSHA integral. Having them pre-computed allows to immediately check in real-time the decisional rule of Eq. (17.5).

**Table 17.1** Exceedance probability for an arbitrary  $PGA_c$  value of 0.017 g as a function of the only two parameters required to compute the RTPSHA integral, showing offline computability

n = 18	Estimated source-to-site distance; i.e., modal value of the PDF of R (km)					
$\hat{\tau}$ [s]	50	70	90	110	130	150
0.2	0.0363	0.0053	0.0009	0.0002	0.0000	0.0000
0.4	0.0442	0.0069	0.0012	0.0003	0.0001	0.0000
0.6	0.1338	0.0351	.0098	0.0030	0.0010	0.0003
0.8	0.6085	0.3423	0.1795	0.0925	0.0479	0.0251
1.0	0.9240	0.7737	0.5949	0.4331	0.3055	0.2117
1.2	0.9912	0.9548	0.8814	0.7801	0.6669	0.5552
1.4	0.9990	0.9919	0.9700	0.9279	0.8661	0.7897
1.6	0.9998	0.9973	0.9875	0.9643	0.9245	0.8689
1.8	0.9999	0.9984	0.9917	0.9744	0.9425	0.8953
2.0	0.9999	0.9988	0.9933	0.9783	0.9499	0.9068

The decisional rule allows to define what false (FA) and missed (MA) alarms are; i.e., if the decision, whichever it is, results to be wrong. In the case of the rule of Eq. (17.5) these definitions become Eq. (17.7).

$$\begin{cases} MA : \{Pr [IM > im_c] < Pr_c \cap im > im_c\} \\ FA : \{Pr [IM > im_c] > Pr_c \cap im < im_c\} \end{cases} \quad (17.7)$$

In other words a MA [FA] occurs when the risk, that the critical IM level is going to be exceeded, is too low [high] to issue [to not issue] the alarm, while the actual IM occurring at the site is higher [lower] than  $im_c$ . Consequently, false and missed alarms probabilities,  $P_{FA}$  and  $P_{MA}$ , which are dependent on the time when the decision is supposed to be taken, may be computed; see Iervolino et al. (2006, 2009) for details. An example, referring to the simulation of Fig. 17.2 for some arbitrary  $PGA_c$  values and when  $Pr_c$  is equal to 0.2, is given in Fig. 17.3b. Two important result emerge

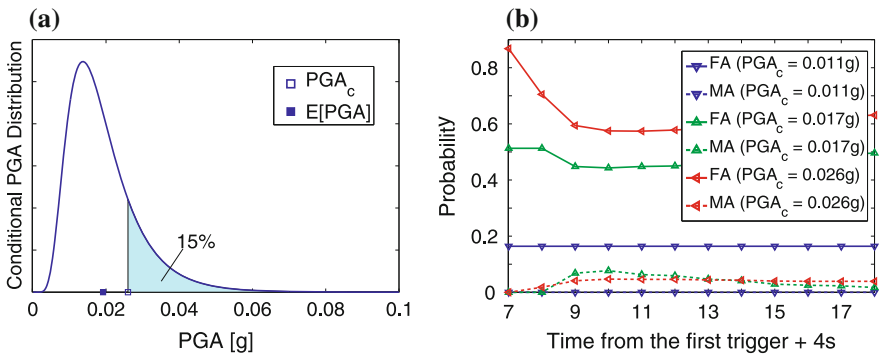


**Fig. 17.3** Representation of decisional rules (a) and examples of false and missed alarm probabilities as a function of time for different IM values (b)

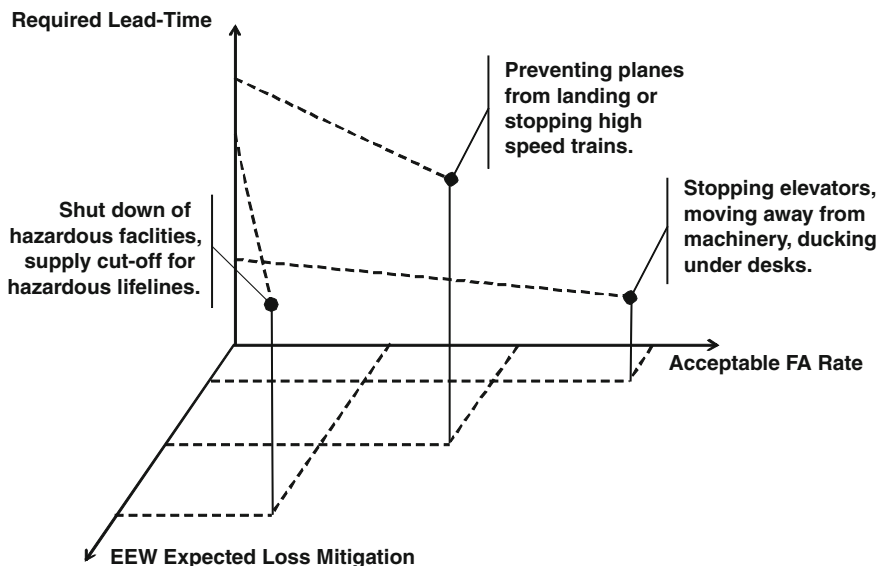


Fig. 17.4 Impact of missed/false alarms for categories of EEW applications; modified from Iervolino et al. (2007b)

from the plots: (1) after a certain  $t$  value the probabilities stabilize, this reflects the fact that after a certain instant the information about the real-time hazard does not change anymore (see following section); (2) there is a trade-off, that is, one can play with  $Pr_c$  and  $im_c$  to lower  $P_{FA}$ , but this always implies that  $P_{MA}$  is going to increase, and vice-versa.

The careful evaluation of the false alarm (or *cry wolf*) probability is increasingly important as the cost associated to the alarm, or to the following security action, raises. In fact, in those cases when the alarm has neither costs nor undesired consequences, the optimal solution is to issue the alert whenever an earthquake event is detected by the EEW system. Conversely, if the alarm may cause costly downtime or affects large communities (e.g., in the case of emergency stop of power plants or lifelines' distribution networks) the alarm decision conditions have to be carefully evaluated to prevent, in the long run, the loss related to false alarms to be unacceptably large. In Fig. 17.4 simple scheme linking three important design variables of engineering earthquake early warning are shown for three different possible EEW applications (relative position with respect to the axes were arbitrarily given).

In the figure it is shown that there are security actions that require a limited lead-time and have a low impact, then a larger FA rate is accepted with respect to actions affecting a larger part of the community more costly, time consuming to operate and for which, then, false alarms are less tolerable (Goltz 2002).

It is to mention that decisional rules based on a ground motion IM thresholds, as those presented, have the advantage to be simple and requiring limited information of the structure to alert (i.e., those required to set  $im_c$ ). However, the IM is only a proxy

for the loss associated to the earthquake hitting the structure. In fact, the alarming decision should be better taken comparing in real-time the expected losses consequent the decision to alarm or to not alarm, conditional on the available information about the impending earthquake. This has been investigated in Iervolino et al. (2007a) and is briefly discussed in the following.

### 17.2.3 ERGO: An Example of RTPSHA Terminal

The *EaRly warninG demo* (ERGO) was developed to test the potential of hybrid EEW based on RTPSHA. The system was developed by the staff of the *RISSC Lab* ([www.rissclab.unina.it](http://www.rissclab.unina.it)). ERGO processes in real-time the accelerometric data provided by a sub-net (6 stations) of ISNet and is installed in the main building of the school of engineering of the University of Naples Federico II, in Naples, which is the target site of the EEW. It is able to perform RTPSHA and eventually to issue an alarm in the case of potentially dangerous events occurring in the southern Appennines region. ERGO is composed of the following four panels (Fig. 17.5).

- *Real-time monitoring and event detection:* In this panel two kind of data are given: (a) the real-time accelerometric signals of the stations, shown on a two minutes time window; and (b) the portion of signal that, based on signal-to-noise ratio, determined the last trigger (i.e., event detection) of a specific station (on the left). Because it may be the case that local noise (e.g., veicular traffic) determines a station to trigger, the system declares an event (M larger than 3) only if at least three station trigger within the same 2 s time interval.
- *Estimation of earthquake parameters:* This panel activates when an event is declared. If this condition occurs, magnitude and location are estimated in real-

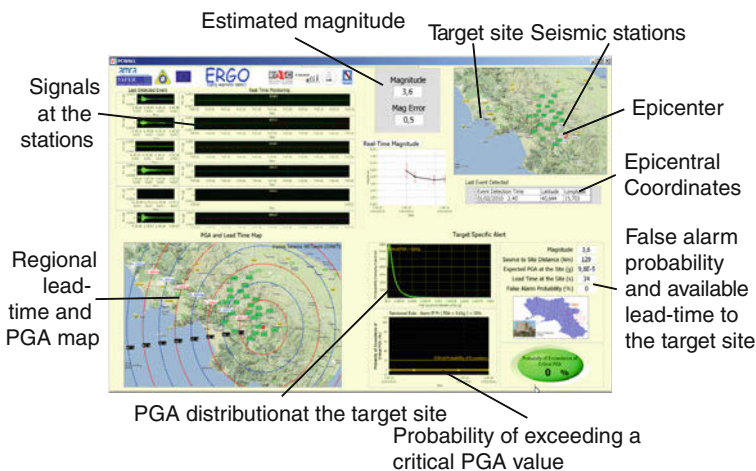


Fig. 17.5 ERGO, a RTPSHA-based early warning terminal

time as a function of evolving information from the first panel. Here the expected value of magnitude as a function of time and the associated standard error are given. Moreover, on a map where also the stations are located (rectangles), it shows the estimated epicenter (red circle), its geographical coordinates and the origin time.

- *Lead-time and peak-shaking map:* This panel shows the lead-time associated to S-waves for the propagating event in the whole region. As further information, on this panel the expected PGA on rock soil is given on the same map. As per the second panel, this one activates only if an event is declared from panel 1 and its input information come from panel 2.
- *RTPSHA and alarm issuance decision:* This panel performs RTPSHA for the site where the system is installed based on information on magnitude and distance from panel 2. In particular, it computes and shows real-time evolving PDFs of PGA at the site. Because a critical PGA value has been established (arbitrarily set equal to 0.01 g) the system is able to compute the risk this PGA is exceeded as a function of time. If such a risk exceeds 0.2, the alarm is issued and an otherwise green light turns to red, as per Eq. (17.5). This panel also gives, as summary information, the actual risk that the critical PGA value is exceeded along with the lead-time available and the false alarm probability.

Figure 17.5 refers to a real event detected and processed in real-time by ERGO on February 01 2010. The system estimated the event as an M 3.6, with an epicenter about 130 km far from the site. Because the event was a low-magnitude large-distance one, the risk the  $PGA_c$  could be exceeded was negligible and the alarm was, correctly, not issued. Finally, note that ERGO is a visual panel only for demonstration and testing purposes, but it may be virtually ready be connected to devices for real-time risk reduction actions.

### ***17.2.4 Uncertainties in EEW Ground Motion Predictions and Information-Dependent Lead-Time***

Three different sources of uncertainty affect the IM estimation according to Eq. (17.3), that is, those related to the estimation of M, R, and IM given M and R. Except for the PDF of IM given M and R, the uncertainty involved is time-dependent because the uncertain estimations of magnitude and distance are also time-dependent. A great deal of research has focused on the fine tuning of the estimation of M and related uncertainty; however in the RTPSHA ground motion prediction uncertainty, that on M is not the weak link. This is proven in Iervolino et al. (2009) from where Fig. 17.6a is taken. It shows, for the M 6 event simulated in Fig. 17.2 the coefficient of variation (CoV, the ratio of the standard deviation to the mean) of the PGA prediction is given as the time from the origin time of the earthquake and number of stations providing  $\tau$  (the information about the source parameters of the impending earthquake) increase. This may be seen as a measure of the evolving uncertainty on EEW ground motion prediction, and it may be recognized to be significantly large (never below 0.45),

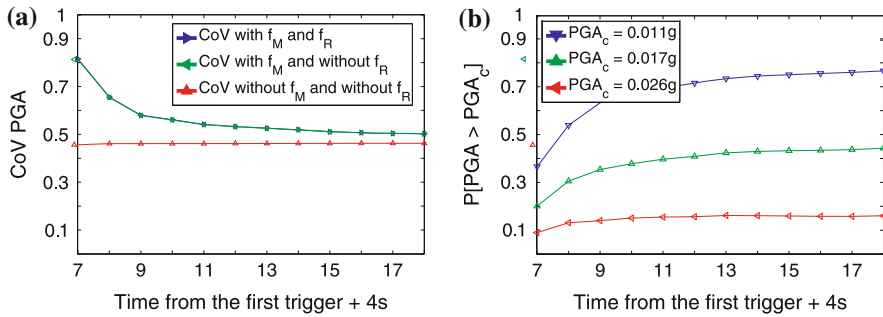


**Fig. 17.6** Coefficient of variation of the IM PDFs when different uncertainties are considered (a), and dependence of IM estimations as a function of time (b); adapted from Iervolino et al. (2009)

at least in this example. This means that alarming decisions based on this approach may be taken in very uncertain conditions, and this is because of the IM given  $M$  and  $R$  (i.e., the GMPE). In fact, in the figure the CoV is computed, using Eq. (17.3) at any 1s step from the earthquake origin time, in the following cases:

- considering both PDFs of  $M$  and  $R$ ;
- considering the PDF of  $M$  and only the modal value of the distance ( $R^*$ ) from Fig. 17.2d in place of its full PDF;
- neither the PDF of  $M$  nor of  $R$ , while using two statistics as the mode of  $R$  and the maximum likelihood value of magnitude ( $\bar{M}$ ).

Case (a) corresponds to fully apply the RTPSHA approach; in case (b) only the uncertainty on  $M$  reflects on the real-time PGA prediction; and in (3) neither uncertainty related to the estimation of  $M$  nor of  $R$  affect the estimation of PGA, and at any instant the real-time hazard is simply given by  $f(im|m, r)$ . In this latter case the uncertainty is only that of the GMPE computed for the specific  $\{\bar{M}, R^*\}$  pair.

It clearly appears from the curves that the uncertainty of the distance is negligible with respect to the prediction of PGA because green and blue curves are overlapping, meaning that the CoV of PGA is almost the same with or without uncertainty on distance. Also the contribution of uncertainty of magnitude to the CoV of PGA is small if compared to that of the GMPE, except at the beginning when the estimation of  $M$  is not yet well constrained by several  $\tau$  measurements. Unfortunately, the GMPE uncertainty, which largely dominates, is not dependent on the measures in the described RTPSHA approach. (Therefore, it seems that possible attempts reduce uncertainty in EEW ground motions predictions may only refer to random field modeling of spatial IM distribution, as discussed in Iervolino (2011)).

Because this time dependence of the  $M$  and  $R$  estimations, the prediction of IM becomes stable only after a number of stations have measured the early signal of the event. This is better shown in Fig. 17.6b where the estimation of the exceedance probability for three hypothetical  $PGA_c$  values, to be used in one of the decisional rules discussed, is given as a function of time (note that  $t$  equal to 7, 13 and 18s correspond to Fig. 17.2a–c, respectively).

It appears that the probability of exceedance does not change after 10–13 s, independently of which  $PGA_c$  value is considered. In other words, after on average 11–18 stations of the ISNet have measured  $\tau$ , the estimation of the critical PGA does not benefit much from further information. It may be concluded that there is a trade-off between the lead-time and the level of information based on which the alarm issuance is decided. Consequently, different lead-times may be computed for the Campania region, each of those corresponds to a different number of stations providing  $\tau$ , for example 4, 18 and 29 representing three levels of information about the source of the earthquake: *poor*, *large*, and *full*, respectively (Fig. 17.7); see Iervolino et al. (2009) for details.

Because 18 stations is the minimum level of information to stabilize the uncertainty, the 18-station average lead-time map can be considered as the reference for the design of real-time risk reduction actions, some of which from Goltz (2002) are superimposed in Fig. 17.8.

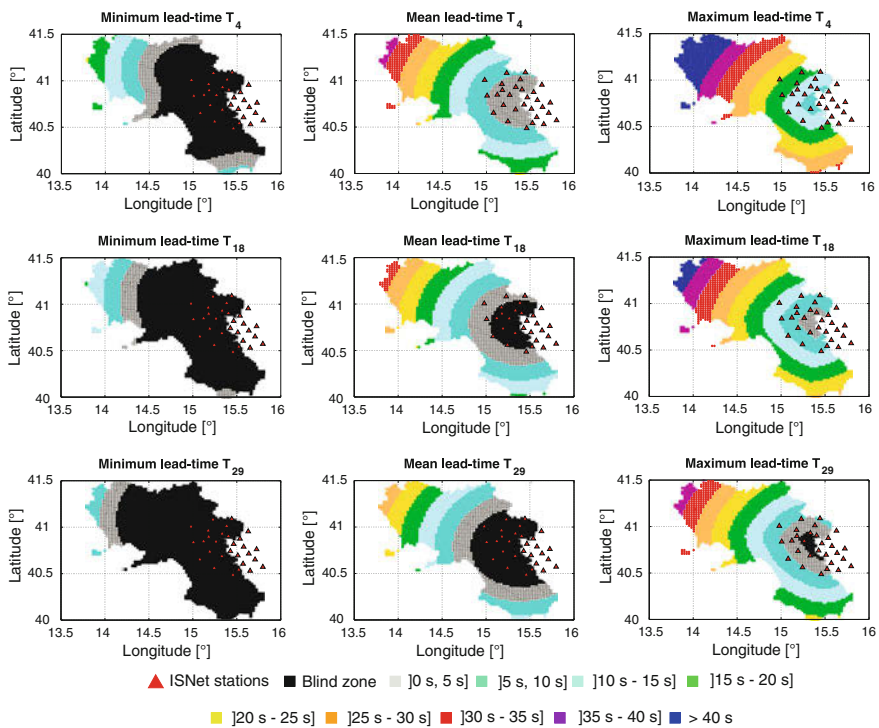


**Fig. 17.7** Minimum, mean and maximum lead-time maps for random hypocenters when 4, 18 and 29 ISNet stations have provided information to estimate the magnitude

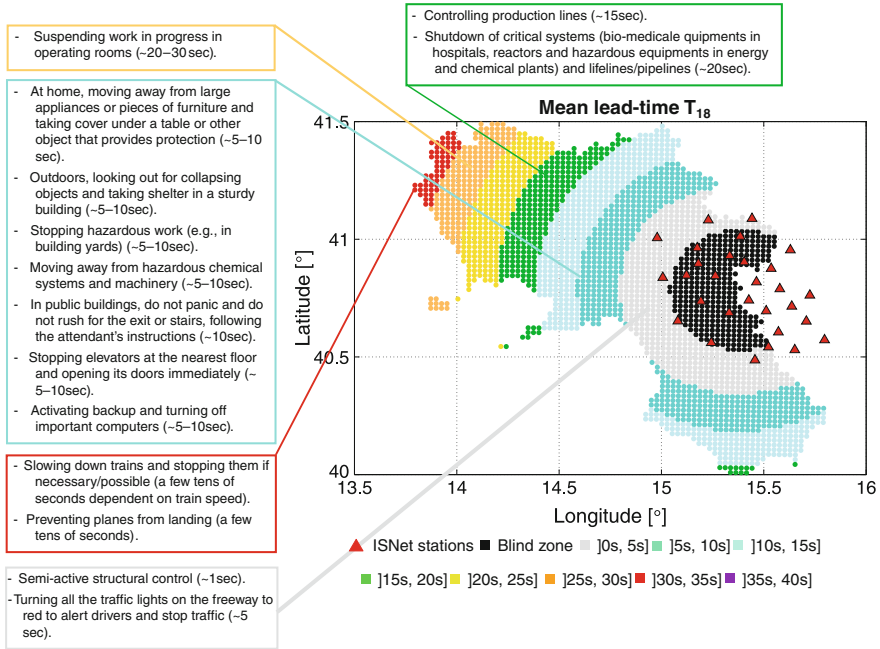


**Fig. 17.8** Design lead-time map for the Campania region (southern Italy); modified from Iervolino et al. (2009)

### 17.3 Estimating Earthquake Consequences for Structures in Real-Time

The real-time prediction of a ground motion IM discussed so far, although the first step from real-time seismology to structural performance, is neither the best option to estimate the damage potential for a specific structure nor the more appropriate piece of information on the basis of which to decide whether to alarm. In fact, it is well known that the IM maybe only poorly correlated to the structural seismic response and that different damages occurring in a building (e.g., to structural components, to non-structural components, and to content) may require the estimation of more than one IM at the same time. In other words, if one is able to quantify the damages (i.e., the loss) specific for the structure of interest this is a sounder basis for the warning management. This structure-specific EEW design procedure was investigated in Iervolino et al. (2007a) where it was shown with respect to the issue of calibrating an alarm threshold which is *optimal* in the sense of minimizing the losses, including the false and missed alarm related costs. Such an approach is briefly reviewed in the following.

The performance-based seismic risk assessment of structures aiming to the estimation of the mean annual frequency of certain loss ( $L$ ) may be adapted to the EEW

real-time case as done for the RTPSHA. In fact, for a structure provided of an EEW terminal such as ERGO, the expected loss may be computed in the case of warning issuance ( $W$ ) and no alarm issuance ( $\bar{W}$ ) as follows:

$$E^W [L|\underline{\tau}, \underline{s}] = \int_L \int_{DM} \int_{EDP} \int_{IM} l f^W(l|\underline{dm}) f(\underline{dm}|\underline{edp}) \times f(\underline{edp}|\underline{im}) f(\underline{im}|\underline{\tau}, \underline{s}) dL dDM dEDP dIM \quad (17.8)$$

$$E^{\bar{W}} [L|\underline{\tau}, \underline{s}] = \int_L \int_{DM} \int_{EDP} \int_{IM} l f^{\bar{W}}(l|\underline{dm}) f(\underline{dm}|\underline{edp}) \times f(\underline{edp}|\underline{im}) f(\underline{im}|\underline{\tau}, \underline{s}) dL dDM dEDP dIM \quad (17.9)$$

where the terms the two equations share are:  $f(l|\underline{dm})$  which is the PDF of the loss given the vector of structural and non-structural damage measures ( $DM$ );  $f(\underline{dm}|\underline{edp})$  or the joint PDF of damages given the engineering demand parameters ( $EDP$ ), proxy for the structural and non-structural response;  $f(\underline{edp}|\underline{im})$  or the joint PDF of the EDPs is generally conditional to a vector of ground motion intensity measures ( $IM$ );  $f(\underline{im}|\underline{\tau}, \underline{s})$  is the real-time hazard for the  $IM$  vector of interest (e.g., two IMs one related to structural response and one to non-structural response).

The two equations are different for the loss function term. In other words, it may be assumed that a security action, aimed at risk mitigation, is undertaken if the alarm is issued. For example, some critical system will shut down or people in a school building may duck under desks if the warning time is not sufficient to evacuate.<sup>4</sup> In fact,  $f^W(l|\underline{dm})$  is the loss reflecting the risk reduction; and  $f^{\bar{W}}(l|\underline{dm})$  is the loss function if no alarm is issued (no security action is undertaken).

In the case it is possible to compute, before the ground motion hits, the expected losses in case of warning or not, clearly one can take the optimal decision: to alarm if this reduces the expected losses and to not issue any warning otherwise, Eq. (17.10).

$$\begin{cases} \text{to alarm if} & E^W [L|\underline{\tau}, \underline{s}] \leq E^{\bar{W}} [L|\underline{\tau}, \underline{s}] \\ \text{to not alarm if} & E^W [L|\underline{\tau}, \underline{s}] > E^{\bar{W}} [L|\underline{\tau}, \underline{s}] \end{cases} \quad (17.10)$$

The described approach was pursued for a simplified school building consisting of one classroom (Fig. 17.9), in which three kinds of losses were considered, the assumed occurrence of which is summarized in Table 17.2.

<sup>4</sup> More complex security measures may be related to the semi-active control of buildings; e.g. Iervolino et al. (2010) and Fujita et al. (2011).

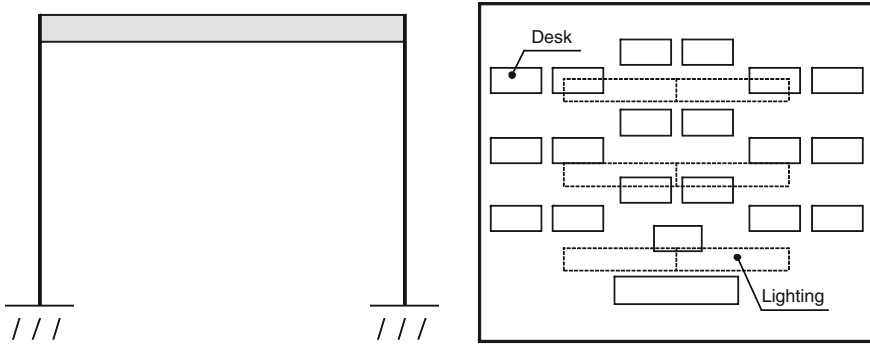


**Fig. 17.9** Structural scheme for the school building (**left**), and classroom layout (**right**); modified from Iervolino et al. (2007a)

**Table 17.2** Losses considered and occurrence cases

Loss	Structural collapse	Non-structural damage only	Neither structural nor non-structural damage
Costs due to casualties and injuries	<i>Occurs</i>	<i>May occur (in a reduced manner in the case of warning)</i>	<i>Does not occur</i>
Cost due to structural reparation and re-construction	<i>Occurs</i>	<i>Does not occur</i>	<i>Does not occur</i>
Costs related to downtime	<i>Occurs</i>	<i>Occurs</i>	<i>Occurs in the case of warning</i>

The costs of casualties and injuries were conventionally assigned in an approach similar to insurance premiums computation. The security action to be undertaken after the alarm issuance was supposed to be ducking of occupants under desks.

To reflect the undertaking of the security action in case of alarm, the loss function was generally reduced with respect to the non-issuance alarm case (Fig. 17.10a). All other terms shared by Eqs. (17.8) and (17.9) were computed via non-linear structural analyses.

With this approach  $E^W [L | \hat{\tau}]$  and  $E^{\bar{W}} [L | \hat{\tau}]$  were calculated for the example under exam considering the ISNet EEW system, for ten equally spaced  $\hat{\tau}$  values in the range between 0.2 and 2s and assuming  $n = 29$ ; i.e., it is assumed that all stations of the ISNet have measured  $\tau$ . Because it has been discussed that the localization method involves negligible uncertainty, the R value has been fixed to 110km which is a possible distance of a building in Naples for an event having its epicentral location in the Irpinian region. In Fig. 17.10b the trends of the expected losses in the two cases are given, the black curve (dashed and solid) corresponds to the non-issuance of the alarm, the red one refers to the issuance. The intersection

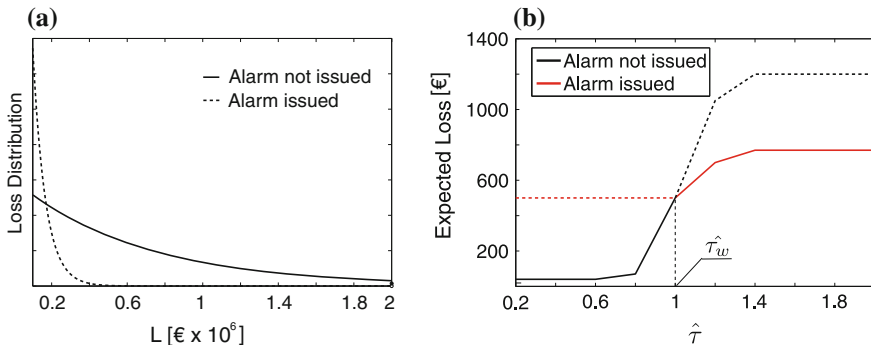


**Fig. 17.10** Loss PDF when the alarm is not issued and when it is reduced because ducking under desks after the alarm is issued (a), and expected loss as a function of the measures used to estimate the magnitude in real-time with identified optimal alarm threshold (b); modified from Iervolino et al. (2007a)

of the two curves defines two  $\hat{\tau}$  regions and the optimal alarm threshold ( $\hat{\tau}_w$ ); if the statistic of the measurements is below the intersection value the expected loss is lower if the warning is not issued, otherwise, if  $\hat{\tau} > \hat{\tau}_w$ , the optimal decision is to alarm because it minimizes the expected loss.

To determine the alarm threshold based on the expected loss allows to account for all actual costs related to the event striking and the alarm consequences probabilistically, and it is easy to recognize how this is an improvement with respect to synthesize all structural response, damages and consequences in the  $im_c$  threshold discussed above. Moreover, because the loss estimations accounts for false and missed alarms, the threshold is also optimal with respect to the MA and FA tradeoff.

## 17.4 Conclusions

In this paper a performance-based earthquake engineering framework to earthquake early warning was reviewed. The focus is the probabilistic prediction of the structural consequences or losses at a given site based on the information gathered during an earthquake by a seismic network able to process in real-time the recordings.

The first step was the early warning adaption of probabilistic seismic hazard analysis, which allows to predict in real-time any ground motion intensity measure for which a prediction equation is available. As a side results, an analytical form solution for the real-time estimation of magnitude, under some hypotheses, was found based on some fundamental results of real-time seismology. Subsequently, the alarm issuance based on strong motion intensity measures was faced. Possible decisional rules and consequent missed and false alarm probabilities were analyzed.

In the context of site-specific engineering ground motion predictions, it was shown that the GMPE is the largest source of uncertainty in EEW engineering ground motion

prediction with respect to real-time estimate of source parameters as magnitude and location. Similarly, it was shown that because the information (the uncertainty) is time-dependent, the reference time after which the level of information does not increase significantly, while the earthquake has not yet reached all stations within the EEW network, may be identified in EEW systems. Therefore uncertainty-dependent lead-time should be considered as an additional design parameter for engineering EEW applications.

On the structural engineering counterpart, the structural performance and losses may be predicted in real-time, which allow: to evaluate the actual efficiency of security actions, to account explicitly for the cost of false alarms, and to take the alarming decision on a more rational basis for a specific structure; i.e., based on expected losses.

Finally, from this brief review of a possible design approach to structure-specific EEW it emerges that many important issues in engineering earthquake early warning still need to be addressed: first of all the effectiveness and economic convenience with respect to more traditional structural seismic risk mitigation technologies. However, these studies at least prove that EEW deserves attention from earthquake engineering as it is an opportunity to be investigated among advanced and cost-effective risk management approaches.

**Acknowledgments** The author would like to explicitly express his gratitude to coworkers who essentially contributed to the studies this paper reviews. Moreover, it is to mention that most of the research presented was developed within the funded research programs of AMRA (<http://www.amrcenter.com/>) and the ReLUIIS-DPC (<http://www.reluiss.it/>) 2005–2008 project.

## References

- Allen RM, Kanamori H (2003) The potential for earthquake early warning in Southern California. *Science* 300(5620):786–789
- Convertito V, Iervolino I, Manfredi G, Zollo A (2008) Prediction of response spectra via real-time earthquake measurements. *Soil Dyn Earthq Eng* 28(6):492–505
- Cornell CA (1968) Engineering seismic risk analysis. *Bull Seismol Soc Am* 58(5):1583–1606
- Cornell CA, Krawinkler H (2000) Progress and challenges in seismic performance assessment. *PEER Center News* 3(2):4p
- Doi K (2010) The operation and performance of earthquake early warnings by the Japan meteorological agency. *Soil Dyn Earthq Eng* 31(2):119–126.
- Fujita S, Minagawa K, Tanaka G, Shimosaka H (2011) Intelligent seismic isolation system using air bearings and earthquake early warning. *Soil Dyn Earthq Eng* 31(2):223–230
- Goltz JD (2002) Introducing earthquake early warning in California: a summary of social science and public policy issues, report to OES and the operational areas. Governor's Office for Emergency Service, Pasadena, CA, US. <http://www.cisn.org/docs/Goltz.TaskI-IV.Report.doc>
- Heaton TH (1985) A model for a seismic computerized alert network. *Science* 228(4702):87–90
- Iervolino I (2011) Performance-based earthquake early warning. *Soil Dyn Earthq Eng* 31(2):209–222
- Iervolino I, Convertito V, Giorgio M, Manfredi G, Zollo A (2006) Real time risk analysis for hybrid earthquake early warning systems. *J Earthq Eng* 10(6):867–885
- Iervolino I, Giorgio M, Manfredi G (2007a) Expected loss-based alarm threshold set for earthquake early warning systems. *Earthq Eng Struct Dyn* 36(9):1151–1168

- Iervolino I, Manfredi G, Cosenza E (2007b) Earthquake early warning and engineering application prospects. In: Gasparini P, Manfredi G, Zschau J (eds) Earthquake early warning. Springer, Berlin. ISBN 978-3-540-72240-3.
- Iervolino I, Giorgio M, Galasso C, Manfredi G (2009) Uncertainty in early warning predictions of engineering ground motion parameters: what really matters? *Geophys Res Lett* 36:L00B06. doi:[10.1029/2008GL036644](https://doi.org/10.1029/2008GL036644).
- Iervolino I, Galasso C, Manfredi G (2010) Preliminary investigation on integration of semi-active structural control and earthquake early warning. Early warning system for transport lines workshop, KIT Science Report, Karlsruhe, Germany, ISSN 1619-7399.
- Kanamori H (2005) Real-time seismology and earthquake damage mitigation. *Annu Rev Earth Planet Sci*, 3:5.1-5.20.
- Sabetta F, Pugliese A (1996) Estimation of response spectra and simulation of nonstationarity earthquake ground motion. *Bull Seismol Soc Am* 86(2):337-352
- Satriano C, Lomax A, Zollo A (2008) Real-time evolutionary earthquake location for seismic early warning. *Bull Seismol Soc Am* 98(3):1482-1494
- Veneziano D, Papadimitriou AG (1998) Optimization of the seismic early warning system for the Tohoku Shinkansen. In: Proceedings of 11th European conference on earthquake engineering, Paris, France.
- Wald JD, Quitoriano V, Heaton TH, Kanamori H, Scrivner CW, Orden BC (1999) TriNet "ShakeMaps": rapid generation of peak ground motion and intensity maps for earthquake in Southern California. *Earthq Spectra* 15(3):537-555
- Weber E, Convertito V, Iannaccone G, Zollo A, Bobbio A, Cantore L, Corciulo M, Di Crosta M, Elia L, Martino C, Romeo A, Satriano C (2007) An advanced seismic network in the southern Apennines (Italy) for seismicity investigations and experimentation with earthquake early warning. *Seismol Res Lett* 78(6):622-634
- Wieland M (2001) Earthquake alarm, rapid response, and early warning systems: low cost systems for seismic risk reduction. Electrowatt Engineering Ltd., Zurich
- Wieland M, Griesser M, Kuendig C (2000) Seismic early warning system for a nuclear power plant. In: Proceedings of 12th world conference on earthquake engineering, Auckland, New Zealand.